

Supercell Propagation and Diagnostic Pressure Equation

Derivation of Diagnostic Pressure Equation

Boussinesq approximated moment equations (neglecting friction and Coriolis force)

$$\frac{du}{dt} = -\frac{1}{\rho_0} \frac{\partial p'}{\partial x} \quad (1a)$$

$$\frac{dv}{dt} = -\frac{1}{\rho_0} \frac{\partial p'}{\partial y} \quad (1b)$$

$$\frac{dw}{dt} = -\frac{1}{\rho_0} \frac{\partial p'}{\partial z} + B \quad (1c)$$

Apply divergence operator $\frac{\partial}{\partial x}(1a) + \frac{\partial}{\partial y}(1c) + \frac{\partial}{\partial z}(1d)$:

$$\frac{\partial}{\partial x} \left[\frac{\partial u}{\partial t} + u \frac{\partial u}{\partial x} + v \frac{\partial u}{\partial y} + w \frac{\partial u}{\partial z} \right] = -\frac{1}{\rho_0} \frac{\partial^2 p'}{\partial x^2}$$

$$\frac{\partial}{\partial y} \left[\frac{\partial v}{\partial t} + u \frac{\partial v}{\partial x} + v \frac{\partial v}{\partial y} + w \frac{\partial v}{\partial z} \right] = -\frac{1}{\rho_0} \frac{\partial^2 p'}{\partial y^2}$$

$$\frac{\partial}{\partial z} \left[\frac{\partial w}{\partial t} + u \frac{\partial w}{\partial x} + v \frac{\partial w}{\partial y} + w \frac{\partial w}{\partial z} \right] = -\frac{1}{\rho_0} \frac{\partial^2 p'}{\partial z^2} + \frac{\partial B}{\partial z}$$

Expand and combine terms and remembering $\frac{\partial u}{\partial x} + \frac{\partial v}{\partial y} + \frac{\partial w}{\partial z} = 0$ we get:

$$\begin{aligned} \frac{1}{\rho_0} \nabla^2 p' = & - \left[\left(\frac{\partial u}{\partial x} \right)^2 + \left(\frac{\partial v}{\partial y} \right)^2 + \left(\frac{\partial w}{\partial z} \right)^2 \right] \\ & - 2 \left[\frac{\partial u}{\partial y} \frac{\partial v}{\partial x} + \frac{\partial u}{\partial z} \frac{\partial w}{\partial x} + \frac{\partial v}{\partial z} \frac{\partial w}{\partial y} \right] + \frac{\partial B}{\partial z} \end{aligned}$$

Diagnostic Pressure Equation

- Diagnostic pressure equation is obtained by taking the divergence of the u, v, w momentum equations and then linearizing

$$\mathbf{S} = \frac{\partial \bar{u}}{\partial z} \vec{i} + \frac{\partial \bar{v}}{\partial z} \vec{j}$$

$$\frac{1}{\rho_0} \nabla^2 p' = - \left[\left(\frac{\partial u'}{\partial x} \right)^2 + \left(\frac{\partial v'}{\partial y} \right)^2 + \left(\frac{\partial w'}{\partial z} \right)^2 \right] - 2 \left(\frac{\partial v'}{\partial x} \frac{\partial u'}{\partial y} + \frac{\partial w'}{\partial x} \frac{\partial u'}{\partial z} + \frac{\partial w'}{\partial y} \frac{\partial v'}{\partial z} \right) - 2 \mathbf{S} \cdot \nabla_{\mathbf{h}} w' + \frac{\partial B}{\partial z}$$

Fluid extension terms

Nonlinear dynamic pressure
perturbation, p_{ani}'

Linear dynamic
pressure
perturbation, p_{ai}'

Buoyancy pressure
perturbation, p_b'

NL

$$\begin{aligned} & 2 \frac{\partial u'}{\partial y} \frac{\partial v'}{\partial x} + 2 \frac{\partial u'}{\partial z} \frac{\partial w'}{\partial x} + 2 \frac{\partial v'}{\partial z} \frac{\partial w'}{\partial y} \\ &= \frac{1}{2} \left[\left(\frac{\partial v'}{\partial x} + \frac{\partial u'}{\partial y} \right)^2 + \left(\frac{\partial v'}{\partial z} + \frac{\partial w'}{\partial y} \right)^2 + \left(\frac{\partial u'}{\partial z} + \frac{\partial w'}{\partial x} \right)^2 \right. \\ & \quad \left. - \left(\frac{\partial v'}{\partial x} - \frac{\partial u'}{\partial y} \right)^2 - \left(\frac{\partial v'}{\partial z} - \frac{\partial w'}{\partial y} \right)^2 - \left(\frac{\partial u'}{\partial z} - \frac{\partial w'}{\partial x} \right)^2 \right] \end{aligned}$$

If we assume pure rotation (no div, deformation) and ignore extension terms (i.e., look at the effect of vertical rotation only), then

$$\nabla^2 p'_{NL} = \frac{\rho_0}{2} \left(\frac{\partial v'}{\partial x} - \frac{\partial u'}{\partial y} \right)^2 = \frac{\rho_0}{2} \zeta'^2$$

Diagnostic Pressure Equation

- Diagnostic pressure equation is obtained by taking the divergence of the u, v, w momentum equations and then linearizing

$$p' \propto \left[\left(\frac{\partial u'}{\partial x} \right)^2 + \left(\frac{\partial v'}{\partial y} \right)^2 + \left(\frac{\partial w'}{\partial z} \right)^2 \right] + 2 \left(\frac{\partial v'}{\partial x} \frac{\partial u'}{\partial y} + \frac{\partial w'}{\partial x} \frac{\partial u'}{\partial z} + \frac{\partial w'}{\partial y} \frac{\partial v'}{\partial z} \right) + 2\mathbf{S} \cdot \nabla_h w' - \frac{\partial B}{\partial z}$$

Fluid extension terms
Nonlinear dynamic pressure
perturbation, p_{dnl}'
Linear dynamic
pressure
perturbation, p_{dl}'
Buoyancy pressure
perturbation, p_b'

- Simplify by neglecting horizontal vorticity, deformation, and fluid extension terms, and rewriting remaining nonlinear term $2 \left(\frac{\partial v'}{\partial x} \frac{\partial u'}{\partial y} \right)$

$$p' \propto -\frac{1}{2} \zeta'^2 + 2\mathbf{S} \cdot \nabla_h w' - \frac{\partial B}{\partial z}$$

p_{dnl}'
"spin term"
 p_{dl}'
 p_b'

Dynamic Vertical PGF

- Dynamic vertical PGF that drives dw/dt (momentum eqn) goes as

$$-\frac{\partial p'_d}{\partial z} \propto \frac{1}{2} \frac{\partial \zeta'^2}{\partial z} - 2 \frac{\partial}{\partial z} (\mathcal{S} \cdot \nabla_h w')$$

Nonlinear dynamic forcing Linear dynamic forcing

- Dynamic forcing (nonlinear+linear) has same order of magnitude as buoyancy forcing for supercells because of strong updraft rotation

Nonlinear Dynamic Forcing

$$\frac{\partial p'_d}{\partial z} \propto -\frac{1}{2} \frac{\partial \zeta'^2}{\partial z}$$

- **Crosswise vorticity dominant environment:**
 - vortex pair forms on flank of updraft by tilting
 - nonlinear forcing creates low pressure in each vortex on flanks of updraft
 $\frac{1}{2} \frac{\partial \zeta'^2}{\partial z} > 0 \therefore \frac{\partial p'_d}{\partial z} < 0$
- Upward-directed PGF_d on updraft flanks below $\max \zeta'^2$ causes updraft to split
- Vortex lines tilt downward in rainy downdraft resulting in 2 vortex pairs
- Updraft of right-moving member propagates toward positive vorticity on right flank.
- Updraft of left-moving member propagates toward negative vorticity on left flank

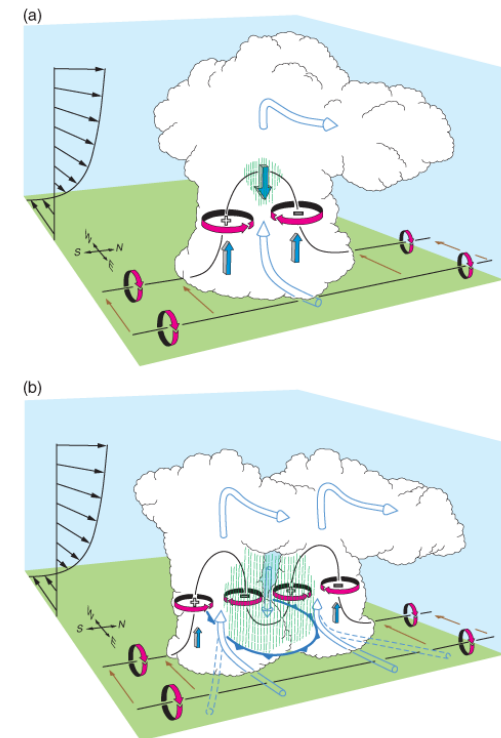


Figure 8.35

The splitting of cells and the subsequent development of rotation through vortex line tilting in the case of a straight hodograph. (a) In the early stage a vortex pair forms through tilting of the horizontal vorticity associated with the mean shear, creating vertical perturbation pressure gradient forces (blue shaded arrows) on the flanks. (b) As rainy downdrafts form and the cell splits, vortex lines are tilted downward, and the original updraft-centered vortex pair is transformed into two vortex pairs. The updraft of the rightward (facing downshear) moving member propagates toward the positive vorticity on the right flank, and thus a correlation between updraft and positive vorticity develops. In (a) and (b), the transparent blue arrows indicate storm-relative trajectories. In (b), the dashed transparent blue arrows indicate storm-relative trajectories after storm splitting. (Adapted from Klemp [1987].)

Source: MR (2010)

Nonlinear Dynamic Forcing

$$\frac{\partial p'_d}{\partial z} \propto -\frac{1}{2} \frac{\partial \zeta'^2}{\partial z}$$

- For pure crosswise vorticity (straight hodograph), forcing leads to upward-directed PGF on flanks of updraft below maximum ζ'^2
 - Storm splitting!
- For pure streamwise vorticity (curved hodograph) vorticity and updraft centered are collocated
 - No storm splitting and right-mover favored!

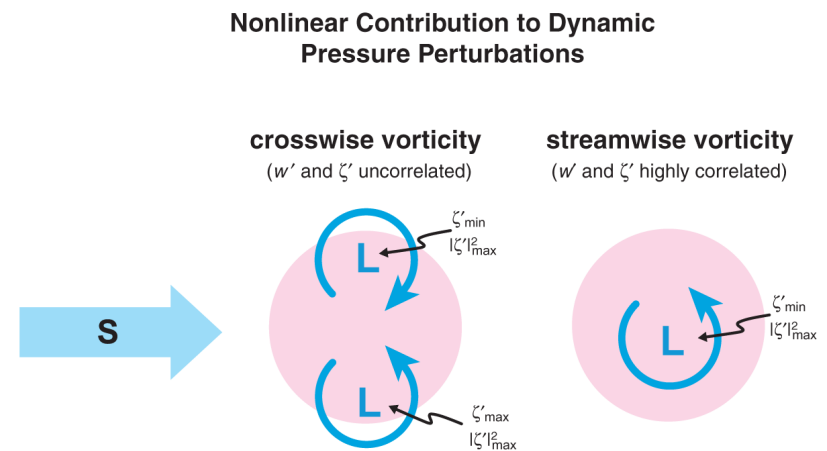


Figure 8.36

Schematic horizontal cross-sections through the midlevel updraft (pink) of a supercell showing the locations of vorticity centers and pressure minima for the cases of purely crosswise vorticity and purely streamwise vorticity. When the vorticity ingested by the updraft is purely crosswise, the $-\frac{1}{2}\zeta'^2$ term in the diagnostic pressure equation leads to an upward-directed dynamic vertical pressure gradient force on the storm flanks below the level of maximum $|\zeta'|$ and minimum p' . In the limit of purely streamwise vorticity being ingested by the updraft, the ζ' and w' fields are approximately in phase; thus, the $-\frac{1}{2}\zeta'^2$ term cannot lead to a significant off-axis, upward-directed, dynamic vertical pressure gradient force.

Nonlinear Dynamic Forcing

$$\frac{\partial p'_d}{\partial z} \propto -\frac{1}{2} \frac{\partial \zeta'^2}{\partial z}$$

- **Straight hodograph (crosswise):**
 - Storm initially moves with mean wind “on the hodograph”
 - After storm splitting, motion of left and right movers are “off the hodograph”
 - Motion “off the hodograph” creates **streamwise vorticity** for right mover and **antistreamwise vorticity** for left mover → mesocyclone and updraft become aligned
- **Curved hodograph (streamwise)**
 - Initial updraft tilts streamwise vorticity from the beginning
 - Storm splitting suppressed
 - Favors cyclonic (anticyclonic) supercell for clockwise (counterclockwise) turning hodograph

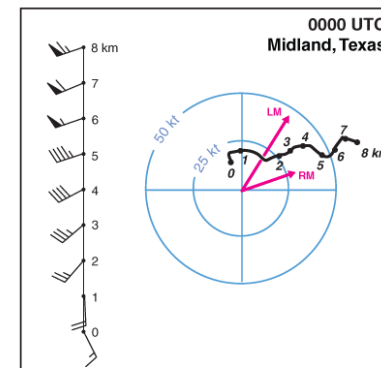
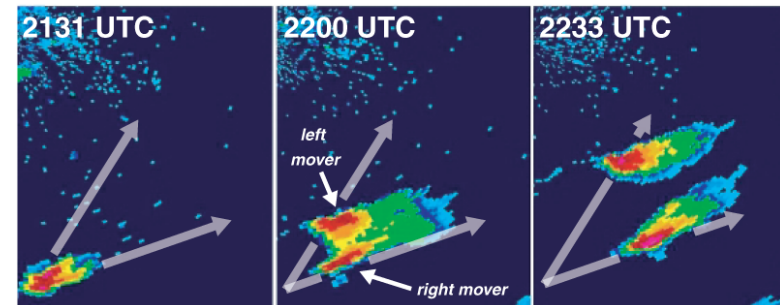


Figure 8.37

Sequence of radar reflectivity images from the Clovis, NM, WSR-88D on 19 April 2004, depicting a developing supercell storm splitting into right- and left-moving supercells. The vertical wind profile and hodograph from Midland, TX, at 0000 UTC 20 April are displayed as well. Numerals along the hodograph indicate altitudes above ground level in kilometers, and the storm motions are also indicated on the hodograph (‘RM’ and ‘LM’ are the motion vectors of the right and left-moving supercells, respectively). The hodograph is fairly straight overall. It is therefore not surprising that the right- and left-moving supercells that developed from the splitting process were comparable in intensity.

Source: MR (2010)

See animation of ARPS simulations:

<https://twister.ou.edu/MM2007/supercell.html>

Linear Dynamic Forcing

$$\frac{\partial p'_d}{\partial z} \propto 2 \frac{\partial}{\partial z} (\mathbf{S} \cdot \nabla_h w')$$

- High (low) pressure is found upshear (downshear) of updraft
- No pressure perturbations on left or right flanks of updraft

Linear Contribution to Dynamic Pressure Perturbations

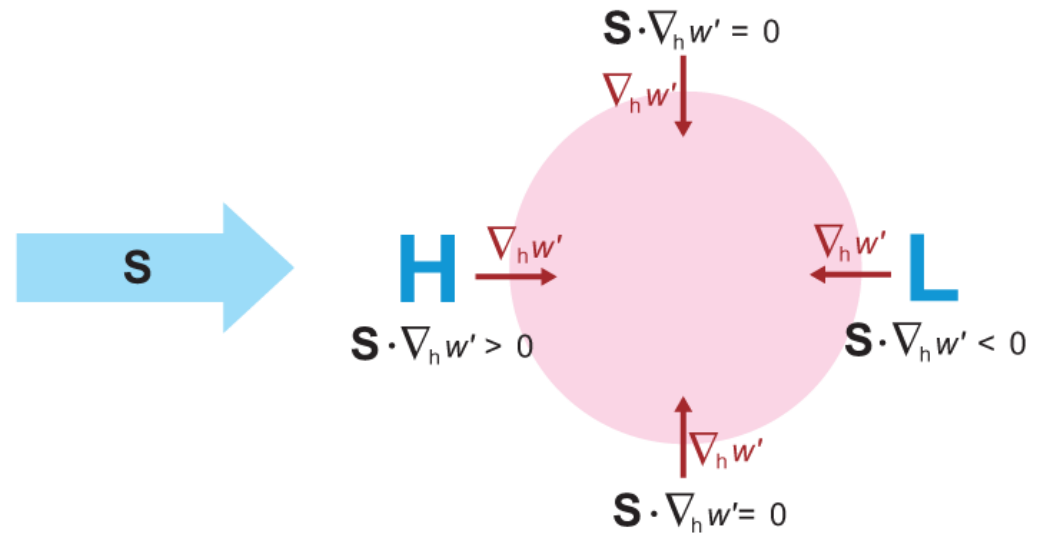


Figure 8.39

Pressure perturbations arising from the linear dynamic term, $2\mathbf{S} \cdot \nabla_h w'$. A couplet of high and low p' is aligned with the shear vector and straddles the updraft at any particular altitude. The magnitude of p' is proportional to the horizontal w' gradient (strong updrafts tend to also have large $\nabla_h w'$) and the strength of the vertical wind shear.

Source: MR (2010)

Linear Dynamic Forcing $\frac{\partial p'_d}{\partial z} \propto 2 \frac{\partial}{\partial z} (\mathbf{S} \cdot \nabla_h w')$

- **Straight hodograph (panel a):**

- **W max is at mid-level**
- **Linear pressure perturbations are vertically stacked**
- **Upward (downward) PGF on downshear (upshear) side of updraft**
- **Horizontal PGF parallel to shear vectors so cannot force lateral (left/right) propagation**

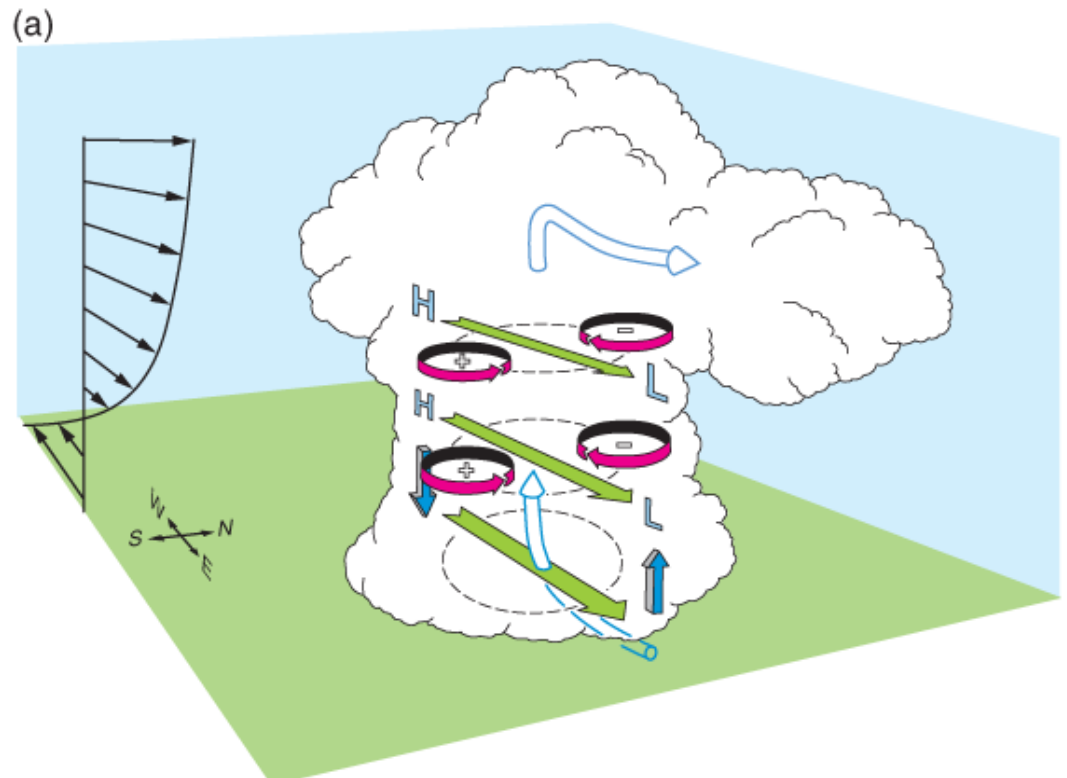


Figure 8.40

Pressure perturbations arising as an updraft interacts with an environmental wind shear that (a) does not change with height and (b) turns clockwise with height. The high (H) to low (L) horizontal pressure gradients parallel to the shear vectors (green flat arrows) are labeled. The dark blue shaded arrows indicate the implied vertical pressure gradient force, which favors the right flank in the curved hodograph case. (Adapted from Klemm [1987].) Source: MR (2010)

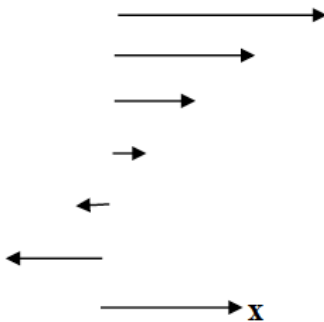
2. Preferred enhancement of right-moving or left-moving storm

Consider the linear p'_{dyn} term:

$$\nabla^2 p' = -\rho_0 \left[2 \frac{\partial \bar{u}}{\partial z} \frac{\partial w'}{\partial x} + \frac{\partial \bar{v}}{\partial z} \frac{\partial w'}{\partial y} \right] = -2\rho_0 \frac{\partial \bar{V}}{\partial z} \cdot \nabla w'$$

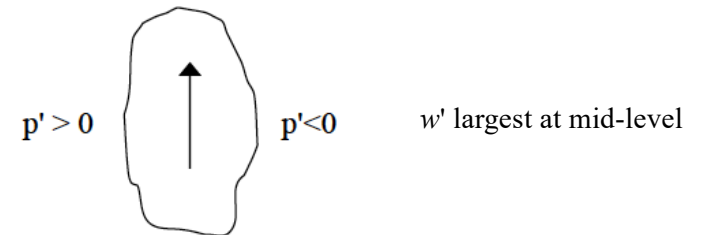
so $p' \propto \frac{\partial \bar{V}}{\partial z} \cdot \nabla w'$. (14)

For unidirectional shear



$$p' \propto \frac{\partial \bar{u}}{\partial z} \frac{\partial w'}{\partial x} > 0 \text{ on the west/upshear flank of updraft}$$

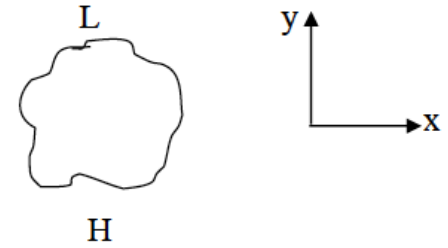
$$p' \propto \frac{\partial \bar{u}}{\partial z} \frac{\partial w'}{\partial x} < 0 \text{ on the east/downshear flank of updraft and } p' \text{ largest at the mid-levels}$$



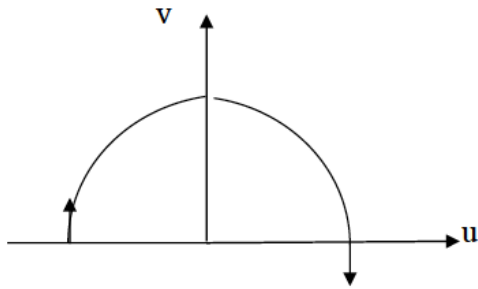
→ new cell growth on the downshear flank

$$\nabla^2 p' = -\rho_0 \left[2 \frac{\partial \bar{u}}{\partial z} \frac{\partial w'}{\partial x} + \frac{\partial \bar{v}}{\partial z} \frac{\partial w'}{\partial y} \right] = -2\rho_0 \frac{\partial \bar{V}}{\partial z} \cdot \nabla w'$$

At low levels, $\frac{\partial \bar{v}}{\partial z} \frac{\partial w'}{\partial y}$, produces



If the hodograph is clockwise curved,

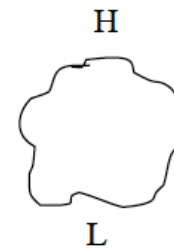


At the mid-levels, $\frac{\partial \bar{u}}{\partial z} \frac{\partial w'}{\partial x}$ produces



then we also have to consider $\frac{\partial \bar{v}}{\partial z} \frac{\partial w'}{\partial y}$ term in (14).

At the upper levels $\frac{\partial \bar{v}}{\partial z} \frac{\partial w'}{\partial y}$ produces



→ there is an upward vertical PGF on the right flank of the storm (downward PGF on the left flank) → new cell growth is enhanced to the right, rotating updraft becomes a 'right mover'.

Linear Dynamic Forcing $\frac{\partial p'_d}{\partial z} \propto 2 \frac{\partial}{\partial z} (\mathbf{S} \cdot \nabla_h \mathbf{w}')$

- **Curved hodograph (panel b):**
 - Vertical PGF is upward on right flank of updraft, favoring right-moving storm
 - Vertical PGF is downward on left flank of updraft, weakening left-moving storm

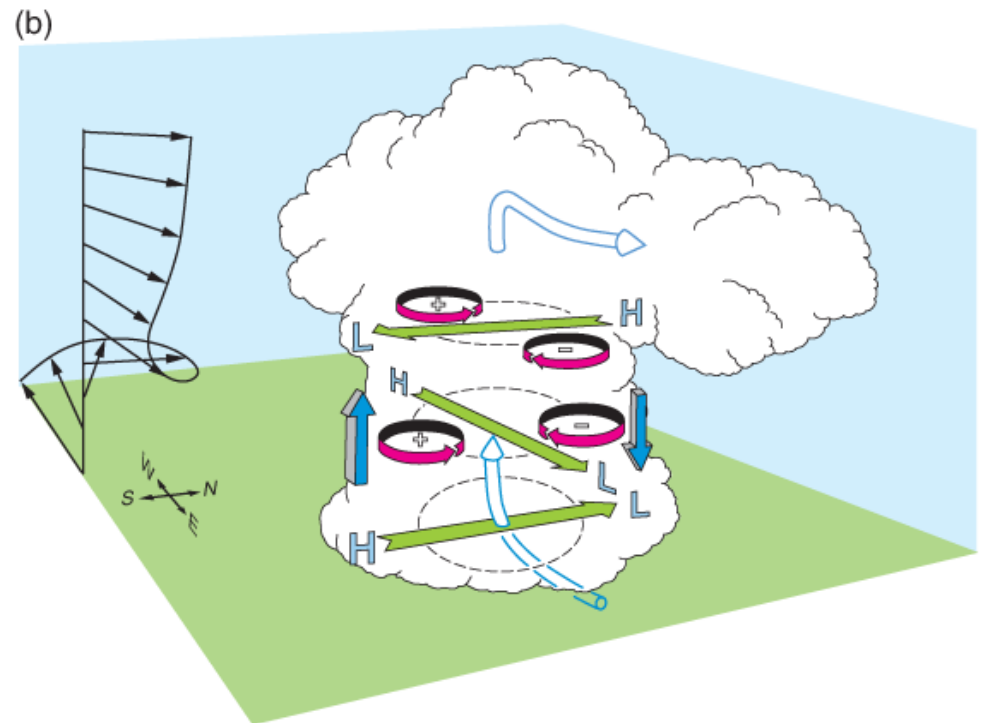
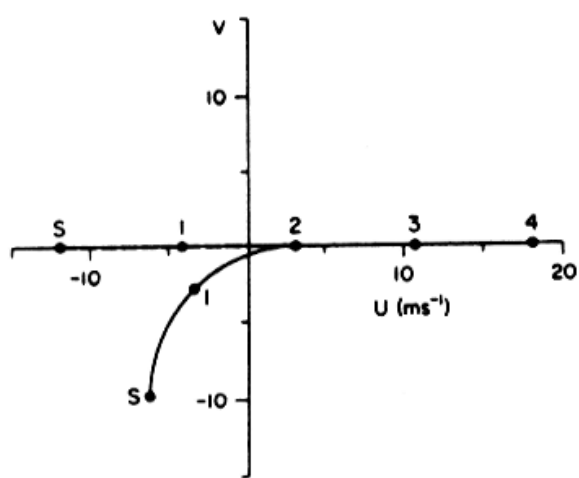


Figure 8.40

Pressure perturbations arising as an updraft interacts with an environmental wind shear that (a) does not change with height and (b) turns clockwise with height. The high (H) to low (L) horizontal pressure gradients parallel to the shear vectors (green flat arrows) are labeled. The dark blue shaded arrows indicate the implied vertical pressure gradient force, which favors the right flank in the curved hodograph case. (Adapted from Klemm [1987].) Source: MR (2010)



(e)

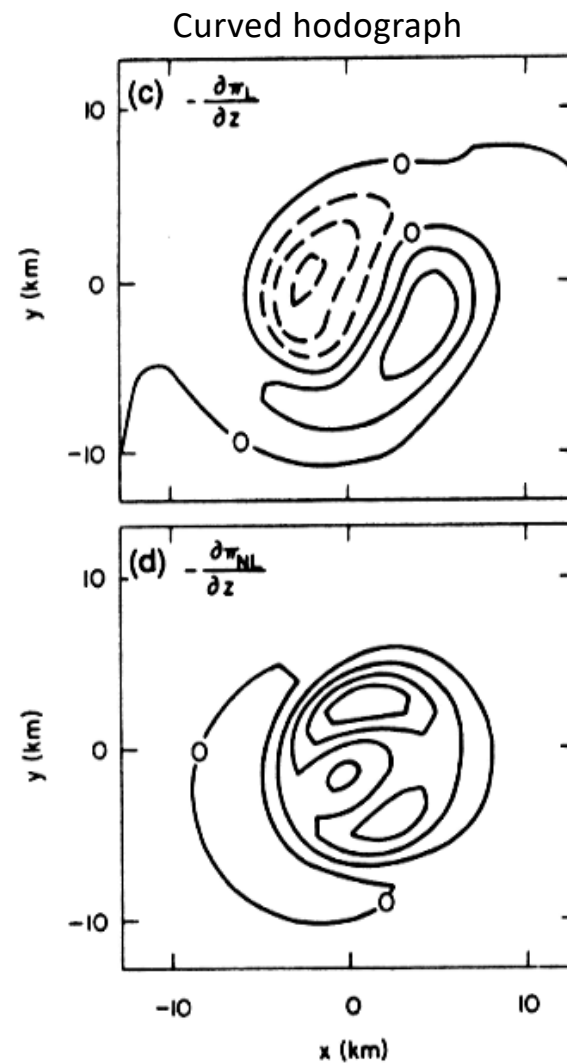
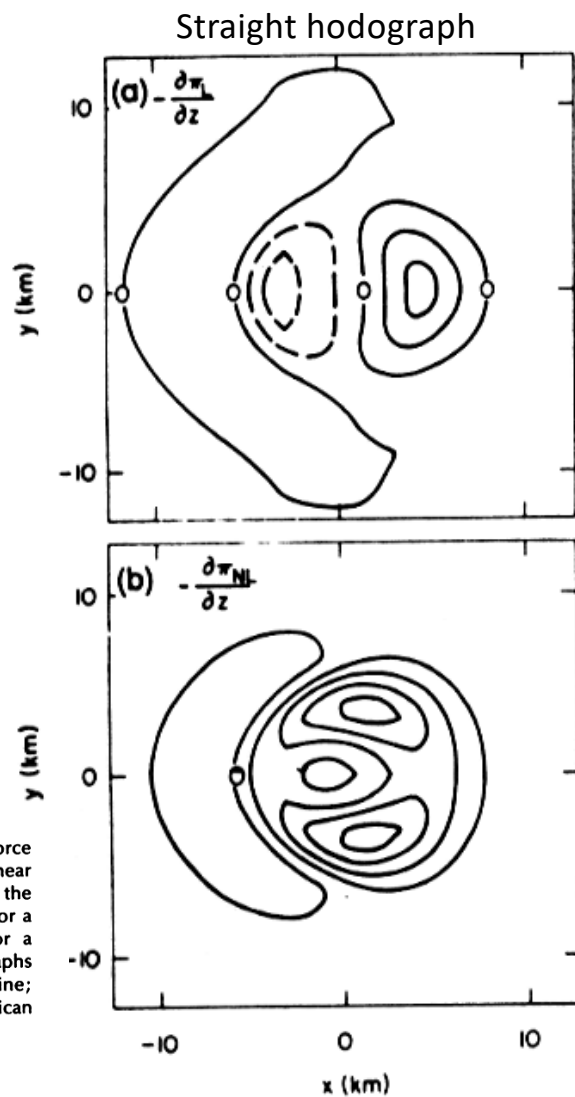
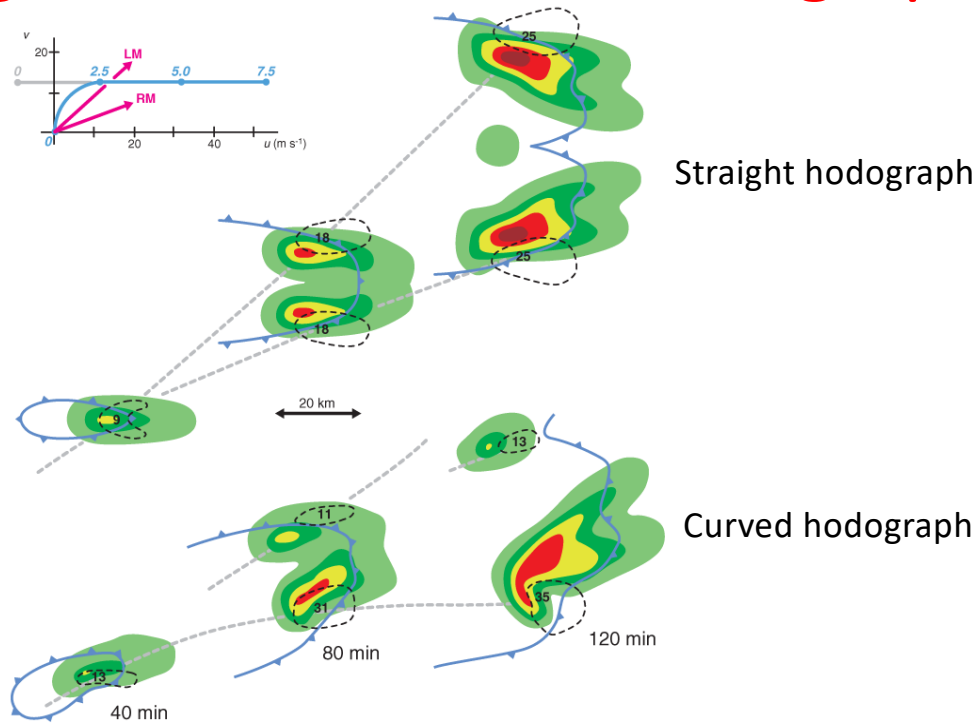


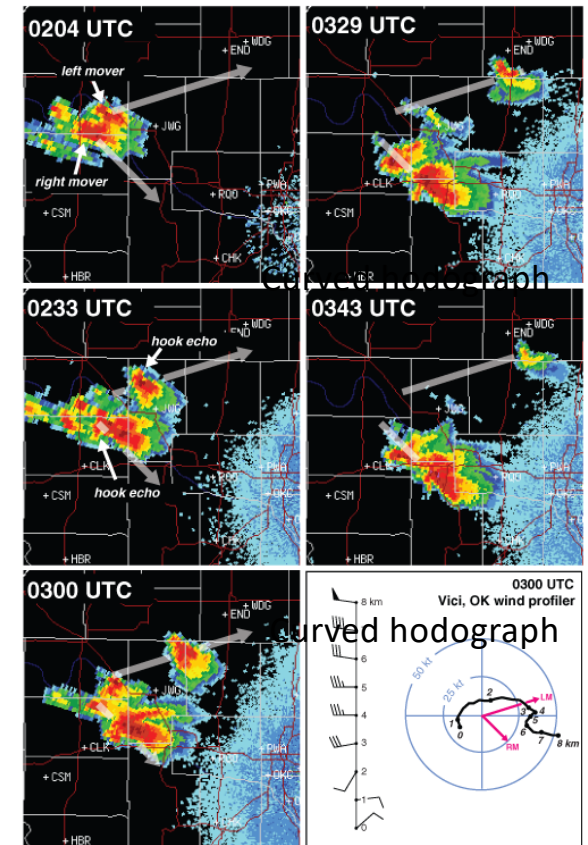
Figure 3.24 Acceleration induced by vertical perturbation-pressure gradient force at 1.5 km in a numerical simulation 10 min after storm initiation for (a) the linear part of the wind field for a straight-line hodograph; (b) the nonlinear part of the wind field for a straight-line hodograph; (c) the linear part of the wind field for a clockwise-turning hodograph; (d) the nonlinear part of the wind field for a clockwise-turning hodograph. Contours plotted every 0.004 m s^{-2} ; (e) hodographs used in the simulations; clockwise-turning hodograph indicated by solid line; heights in km AGL (from Rotunno and Klemp, 1982). (Courtesy of the American Meteorological Society)

Straight versus Curved Hodographs



Plan views of cloud-model-produced, lowlevel rainwater fields for two simulations using, respectively, a straight hodograph (gray in lowest 2.5 km, blue above; numerals along the hodograph indicate altitude in km) and one with low-level clockwise hodograph curvature (blue). The straight hodograph produces storms with mirror-image symmetry, whereas the curved hodograph enhances the right-moving storm. The left- and right-moving storm motions are indicated on the hodographs with magenta arrows and are labeled 'LM' and 'RM', respectively. The dashed black contours enclose the regions of significant midlevel updraft, and the numerals indicate the location and magnitude of the maximum vertical velocity (m s^{-1}). Gust fronts are also shown. The gray dashed lines indicate storm motions. (Adapted from Klemp [1987].)

- **Straight hodograph will result in symmetrical storm splitting**
- **Curved hodograph will result in asymmetrical storm splitting and dominant right mover**



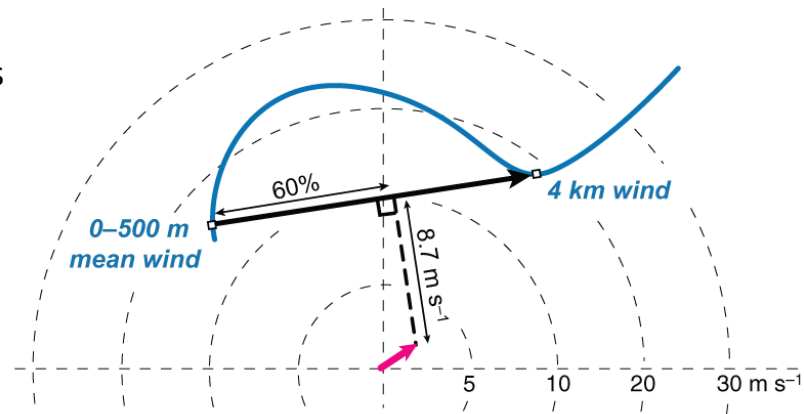
Left- and right-moving supercells following an episode of storm-splitting on 1 June 2008 in western Oklahoma. Note the intensification (weakening) of the right- (left-) mover following the splitting of the original cell. The broad gray arrows indicate the storm motions. The vertical wind profile and hodograph from the nearby Vici, OK, wind profiler are displayed in the bottom right panel. Numerals along the hodograph indicate altitudes above ground level in kilometers, and the storm motions are also indicated on the hodograph ('RM' and 'LM' are the motion vectors of the right and left-movers, respectively). The hodograph has substantial curvature, such that the shear vector veers with height in the lowest 4 km. It is therefore not surprising that the right-mover was dominant in this case.

Source: MR (2010)

Forecasting Supercell Motion

Supercell motion is the result of:

- Downwind advection by mean wind
- Propagation due to dynamic pressure forcing on storm flanks
- Movement of gust front (lesser effect)



Rasmussen and Blanchard (1998) method: Figure 8.43

The Rasmussen and Blanchard (1998) method for forecasting supercell motion predicts a motion 8.7 m s^{-1} orthogonal to the right of a location 60% of the distance from the tail to the head of the shear vector drawn between the 0–500m mean wind and the 4 km wind. In the hodograph, the magenta arrow indicates the predicted supercell motion. Source: MR (2010)

Bunkers et al. (2000) method: motion is 7.5 m/s orthogonal to the right of the shear vector between the 0–500 m mean wind and the 0–6 km mean wind.

Comparison of Supercell Behavior

Property	Straight Hodograph	Strongly Curved Hodograph
Symmetry of left/right movers	Yes	No
Net updraft rotation in initial storm	No	Yes
Cyclonic vortex in initial storm	On right side of updraft	In strong updraft
Anticyclonic vortex in initial storm	On left side of updraft	In downdraft or weak updraft
Storm splitting	Highly significant	Insignificant or absent
Time to first mesocyclone	Slower	Faster
Low and midlevel mesocyclone intensity	Generally less intense	Generally more intense
Mesoanticyclone	In left mover	Generally absent
Max updraft strength	Weaker	Stronger
Direction of low level environment vorticity versus baroclinically generated horizontal vorticity	Very different (roughly orthogonal)	In roughly same direction
Lateral updraft propagation	Via nonlinear dynamic forcing	Via linear dynamic forcing

Good source: A Convective Storm Matrix: Buoyancy/Shear Dependencies (<https://www.meted.ucar.edu/convectn/csmatrix/>)